IJBEM
Vol. 7, No. 2, 2005

Camera-Guided Coordinate System Alignment for Neuromagnetic Source Estimation

Yung-Cheng Cheng[1], Yong-Sheng Chen[2], Jen-Chuen Hsieh[1,3,4,5], and Li-Fen Chen[3,6,*]
[1]Institute of Health Informatics and Decision Making, National Yang-Ming University, Taipei, Taiwan
[2]Department of Computer Science and Information Engineering, National Chiao Tung University, Hsinchu, Taiwan
[3]Lab. of Integrated Brain Research, Dept. of Medical Research and Education, Taipei Veterans General Hospital, Taiwan
[4]Institute of Neuroscience, [5]Faculty of Medicine, [6]Center for Neuroscience, National Yang-Ming University, Taipei, Taiwan

***Abstract*— Coordinate system alignment is usually performed by localizing a set of coils attached to the subject's head in both the coordinate systems of the head and a whole-head neuromagnetometer device. This conventional approach may cause instability of neuronal source localization when the estimated coil positions are not stable or when the coils are not tightly attached. This paper presents a new coordinate system alignment technique without using coils. Instead, the proposed method utilizes a calibrated camera to monitor feature points attached to the subject's face. Coordinate system alignment is then achieved by determining the head pose in neuromagnetometer device coordinate system. According to the phantom experiments, we demonstrate the feasibility, stability, and accuracy of the proposed camera-guided alignment method.**[7]

I. Introduction

Magnetoencephalography (MEG) [1] is a powerful method for in vivo noninvasive imaging of cortical activations. Estimation of neuronal activities requires the information of coordinate transformation between the MEG device and the subject's head coordinate systems. The common way of coordinate system alignment is to attach a set of coils, also called head position indicator (HPI), to the subject's scalp. The coordinates of HPI coils in the head coordinate system can be measured with 3D digitizer in the preparation stage. During the data acquisition stage, small currents are supplied for these coils and their positions in MEG device coordinate system can be determined by dipole fitting from the measured magnetic signals. The transformation between the head and MEG device coordinate systems can then be obtained [2].

Unfortunately, the fitted HPI positions in MEG device coordinate system may be instable. If the HPI coils are not tightly attached to the scalp, their positions may change during the signal acquisition stage because the HPI coils touch the dewar when the subject sits in the MEG system. According to our experience, the measured positions via dipole fitting are not stable even the HPI coils are fixed. Furthermore, this kind of HPI-based method encounters another problem in detecting and correcting head movements in neuromagnetic measurements [3]. The supplied currents for the HPI coils, although in high frequency, may induce interference in the brain network or the MEG measurements. Thus degrades accuracy and correctness of the functional brain imaging from MEG measurements.

In this work, we develop a new coordinate system alignment technique using a camera, instead of HPI coils, as the intermediate. This camera is first calibrated so that the transformation between the camera and MEG device coordinate systems is known and fixed. Then, the subject wears several feature points on her/his face (these feature points will not touch the dewar) during the signal acquisition stage. The camera observes these feature points and the head pose in camera coordinate system can then be determined. Combining the head pose in camera coordinate system and the transformation between the camera and MEG device coordinate systems yields the desired coordinate system alignment between the head and MEG coordinate systems. To have the ground-truth of source positions for accuracy and stability assessment, we performed experiments using phantom data. According to the experiment results, we clearly demonstrate the feasibility, stability, and accuracy of the proposed camera-guided alignment method.

II. Methods

This section describes the procedures of the proposed method for coordinate system alignment in detail. We start with the description of the notations used in this paper.

A. Notations

$\mathrm{C_{MEG}}$, $\mathrm{C_{CAM}}$, $\mathrm{C_{IMG}}$, $\mathrm{C_{OBJ}}$, and $\mathrm{C_{HEAD}}$ represent the coordinate systems of the MEG device, the camera, the image plane in the camera, calibration object, and the subject's head, respectively. In this work, we use a phantom as the calibration object. ${}^{\mathrm{sup}}\mathrm{T}_{\mathrm{sub}}$ denotes the transformation from the sub coordinate system to the sup coordinate system; for instance, ${}^{\mathrm{OBJ}}\mathrm{T}_{\mathrm{MEG}}$ stands for the transformation from the MEG device to calibration object coordinate systems. Here sub and sup could be any one of the above defined five coordinate systems.

B. Overview of the Proposed Method

The goal of this work is to obtain the transformation ${}^{\mathrm{HEAD}}\mathrm{T}_{\mathrm{MEG}}$ used for MEG source estimation. It can be decomposed as follows:

$$ {}^{\mathrm{HEAD}}\mathrm{T}_{\mathrm{MEG}} = {}^{\mathrm{HEAD}}\mathrm{T}_{\mathrm{CAM}}\,{}^{\mathrm{CAM}}\mathrm{T}_{\mathrm{MEG}}. \quad (1) $$

[7]This work is partially supported by Brain Research Center, University System of Taiwan.
*Corresponding author.

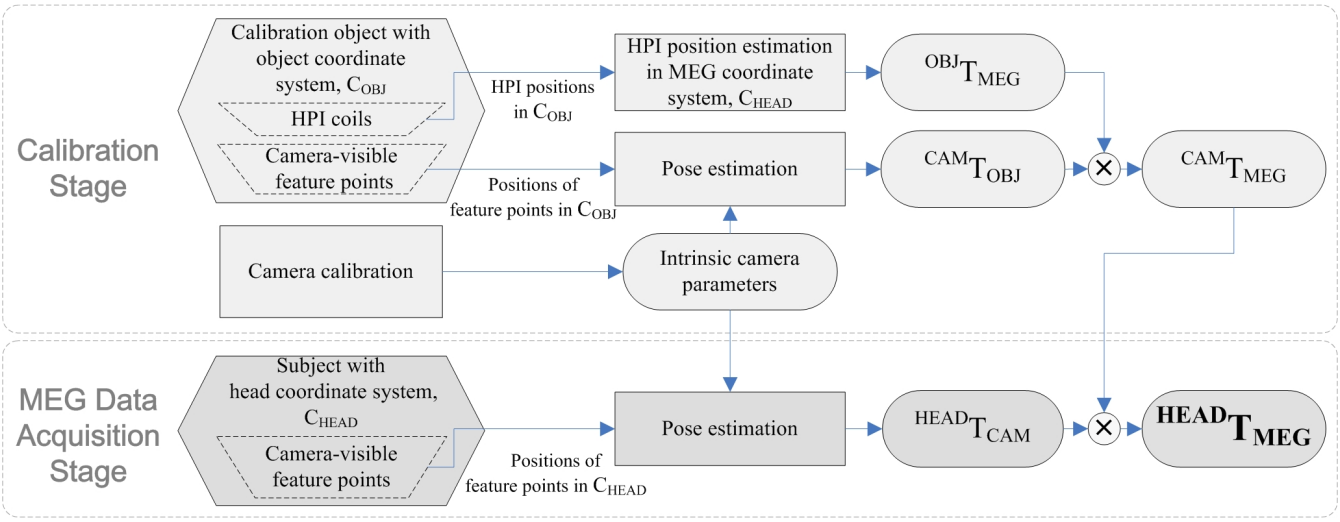

Fig. 1. Illustration of the proposed system schema. The calibration stage is used to estimate all the invariant parameters of the equipments and environment. The MEG data acquisition stage will estimate subject's pose and form the ${}^{\mathrm{CAM}}\mathrm{T}_{\mathrm{MEG}}$ by all the estimated results in both stage.

Once the relative positions between the MEG device and the camera are fixed, the ${}^{\mathrm{CAM}}\mathrm{T}_{\mathrm{MEG}}$ will be invariable.

Based on this concept, the proposed method is composed of two working stages as shown in Fig. 1. All the invariant parameters such as camera intrinsic parameters and ${}^{\mathrm{CAM}}\mathrm{T}_{\mathrm{MEG}}$ can be obtained in the first stage. Camera intrinsic parameters can be estimated by camera calibration techniques. By utilizing the concept of transformation decomposition once more, ${}^{\mathrm{CAM}}\mathrm{T}_{\mathrm{MEG}}$ can be decomposed into the form ${}^{\mathrm{CAM}}\mathrm{T}_{\mathrm{OBJ}}{}^{\mathrm{OBJ}}\mathrm{T}_{\mathrm{MEG}}$. The calibration object is used as a medium for computing ${}^{\mathrm{CAM}}\mathrm{T}_{\mathrm{OBJ}}$ and ${}^{\mathrm{OBJ}}\mathrm{T}_{\mathrm{MEG}}$. A set of camera-visible feature points on the calibration object can be used to estimate ${}^{\mathrm{CAM}}\mathrm{T}_{\mathrm{OBJ}}$ by using pose determination technique. Furthermore, HPI coils attached on the calibration object are used to compute ${}^{\mathrm{OBJ}}\mathrm{T}_{\mathrm{MEG}}$ by using MEG source localization technique. Since subjects are not involved in this stage at all, we refer this stage as calibration, subject-independent stage.

In the second stage, ${}^{\mathrm{HEAD}}\mathrm{T}_{\mathrm{CAM}}$ can be determined by using pose determination technique based on a set of camera-visible feature points on the subject's head. The computation of ${}^{\mathrm{HEAD}}\mathrm{T}_{\mathrm{CAM}}$ is totally device-independent. Once both ${}^{\mathrm{HEAD}}\mathrm{T}_{\mathrm{CAM}}$ and ${}^{\mathrm{CAM}}\mathrm{T}_{\mathrm{MEG}}$ are estimated, ${}^{\mathrm{HEAD}}\mathrm{T}_{\mathrm{MEG}}$ is then obtained.

Among the above mentioned techniques, we describe the process of camera calibration, feature point detection, and pose determination below.

1) Camera Calibration: Intrinsic camera parameters are required to determine the 3-D projection line for each feature points on the captured image. These 3-D projection lines can then be used for pose estimation in the following stage. In this work, we adopt the camera calibration method proposed in [4] due to its simplicity, robustness, versatility, and accuracy. Its widely used implementation in OpenCV library was used to obtain accurate intrinsic camera parameters, including effective focal length, aspect ratio, skew factor, lens distortion, and image center.

2) Feature Point Detection: To reduce the labor of manual feature selection, we use the block matching algorithm to automatically detect the black circles in the image, as shown in Fig. 2. For efficiency, we adopt a fast block matching technique [5] in this work. Once a circle is located, the feature points can be extracted by thresholding [6] the image followed by estimating the centroid.

3) Pose Determination: For a rigid set of 3-D points in the head coordinates, their corresponding feature points projected on the image plane, as well as the intrinsic camera parameters, can be used to determine the pose of the head in the camera coordinate system. At least three points are required for this purpose. In this study, we again use OpenCV library to estimate the head pose, ${}^{\mathrm{CAM}}\mathrm{T}_{\mathrm{HEAD}}$, by using the coordinate pairs of the feature points both in head coordinate system, $\mathrm{C}_{\mathrm{HEAD}}$, and in image coordinate system, $\mathrm{C}_{\mathrm{IMG}}$.

C. System Procedures

The steps of the proposed method are listed as follows:

1) Set up the camera calibration plate as shown in Fig. 2(a) and perform camera calibration for intrinsic parameter estimation.
2) Set up the calibration object as shown in Fig. 2(b) for the first stage.
3) Get the coordinates of HPIs and those of a set of camera-visible feature points in the calibration object coordinate system, $\mathrm{C}_{\mathrm{OBJ}}$, respectively, by using 3D digitizer.
4) Perform location estimation of HPI in the MEG device coordinate system by using MEG dipole fitting technique.
5) Obtain ${}^{\mathrm{OBJ}}\mathrm{T}_{\mathrm{MEG}}$ by using the coordinates of HPIs in both the coordinate systems, $\mathrm{C}_{\mathrm{OBJ}}$ and $\mathrm{C}_{\mathrm{MEG}}$.

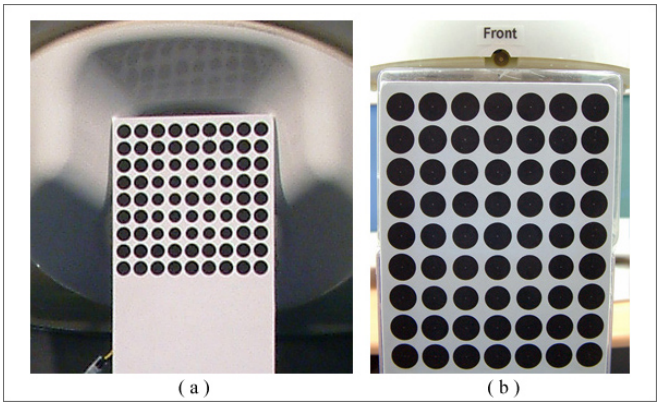

Fig. 2. Two calibration patterns. (a) camera calibration plate; (b) calibration object made by phantom.

6) Perform pose estimation to obtain ${}^{\mathrm{CAM}}\mathrm{T}_{\mathrm{OBJ}}$ by using the 3D coordinates of the feature points in the object coordinate systems, $\mathrm{C}_{\mathrm{OBJ}}$.
7) ${}^{\mathrm{CAM}}\mathrm{T}_{\mathrm{MEG}} = {}^{\mathrm{CAM}}\mathrm{T}_{\mathrm{OBJ}} \times {}^{\mathrm{OBJ}}\mathrm{T}_{\mathrm{MEG}}$.
8) Get the coordinates of camera-visible feature points in the subject's head coordinate system, $\mathrm{C}_{\mathrm{HEAD}}$, by using 3D digitizer.
9) Start MEG data acquisition.
10) Perform pose estimation to obtain ${}^{\mathrm{HEAD}}\mathrm{T}_{\mathrm{CAM}}$ by using the 3D coordinates of the feature points in the subject's head coordinate systems, $\mathrm{C}_{\mathrm{HEAD}}$.
11) ${}^{\mathrm{HEAD}}\mathrm{T}_{\mathrm{MEG}} = {}^{\mathrm{HEAD}}\mathrm{T}_{\mathrm{CAM}} \times {}^{\mathrm{CAM}}\mathrm{T}_{\mathrm{MEG}}$.

III. Experiments

In this study, we use a CCD camera (Marlin, ALLIED Vision Tech. GmbH) with 35 mm focal length lens, 1280×1024 pixel resolution, which is located around 2.1m far from the MEG helmet, with the phantom employed as a subject.

The phantom supplied by the manufactory (Neuromag Ltd., Finland) was used to demonstrate the accuracy of the present work without human intervention. The fixed current dipoles with stationary locations and two-cycle sine waves of duration 120ms were activated individually to generate the electromagnetic field. The peak-to-peak current strength of each dipole was set to 100nAm. Four head position indicator (HPI) coils (fixed on the phantom) were used to obtain the position of the phantom with respect to the sensor array. After well-positioning, the phantom was assumed to keep still within a session. For each session, 100 trials were recorded at a sampling rate of 1000Hz with bandpass filtering 0.1Hz to 333Hz. The preprocessed data were then used for further localization analysis.

In this work, the head conductor was adequately assumed a symmetric spherical model both for the phantom and human brains. The sources of phantom dipole and N20m SEF were modelled by a single ECD model. In the present study, the x, y, z axes indicate the sagittal plane with positive values to the right, the coronal plane with positive values to the front, and the axial plane with positive values up, respectively.

A stability test and a accuracy test will verify our system's performance in the experiment. In the stability test, according to the method in section 2 to estimate the ${}^{\mathrm{CAM}}\mathrm{T}_{\mathrm{MEG}}$, we put the phantom in a fixed orientation, and estimate the ${}^{\mathrm{HEAD}}\mathrm{T}_{\mathrm{MEG}}$ with ten trials through HPI and our system. Then calculate the standard deviation of the results of each system.

In the accuracy test, the phantom dipoles are activated to verify the accuracy of the dipole fitting under the original ${}^{\mathrm{HEAD}}\mathrm{T}_{\mathrm{MEG}}$ through the HPI and another ${}^{\mathrm{HEAD}}\mathrm{T}_{\mathrm{MEG}}$ which is estimated by our system.

The re-projection error of the camera calibration (intrinsic parameters and extrinsic parameters) is 0.1781 pixel. For verifying the stability of the digitizer, we obtain a position of a point by ten times through the digitizer, and the standard deviation of the digitizer is $[0.0568, 0.04830, 0.0667]$ in mm, by x, y, and z axis.

A. The Stability of ${}^{\mathrm{CAM}}\mathrm{T}_{\mathrm{MEG}}$ and ${}^{\mathrm{HEAD}}\mathrm{T}_{\mathrm{MEG}}$

The ${}^{\mathrm{CAM}}\mathrm{T}_{\mathrm{MEG}}$ is a important transformation in our work, because it affects the accuracy and the stability of ${}^{\mathrm{HEAD}}\mathrm{T}_{\mathrm{MEG}}$ estimated by our work. We execute the calibration stage by ten times, and calculate the standard deviation of transformations. Ideally, the ${}^{\mathrm{CAM}}\mathrm{T}_{\mathrm{MEG}}$ should be the same with the related position of the camera and the MEG device fixed. Table I shows that ${}^{\mathrm{CAM}}\mathrm{T}_{\mathrm{MEG}}$ has a little variation (rotation in degree: $[0.2700, 0.0714, 0.1207]$, translation in mm: $[0.1181, 0.2427, 0.2253]$), but the variation of our work is quite small (rotation in degree: $[0.0041, 0.0030, 0.0012]$, translation in mm: $[0.0067, 0.0108, 0.0609]$), so the variation resulted from ${}^{\mathrm{OBJ}}\mathrm{T}_{\mathrm{MEG}}$.

Next, we execute the MEG data acquisition stage by ten times, and calculate the standard deviation of ${}^{\mathrm{HEAD}}\mathrm{T}_{\mathrm{MEG}}$. we take the average value of the ten ${}^{\mathrm{CAM}}\mathrm{T}_{\mathrm{MEG}}$ as a ideal value. As the Table II shows, because the pose estimation of our work is very stable, the standard deviation of our ${}^{\mathrm{HEAD}}\mathrm{T}_{\mathrm{MEG}}$ is more stable than HPI's.

B. The Accuracy of ${}^{\mathrm{HEAD}}\mathrm{T}_{\mathrm{MEG}}$.

After calibration stage, we position the phantom in the MEG device, and execute meg data acquisition once to estimate ${}^{\mathrm{HEAD}}\mathrm{T}_{\mathrm{MEG}}$. Then we activate twelve dipole of phantom to demonstrate the accuracy of dipole fitting under different ${}^{\mathrm{HEAD}}\mathrm{T}_{\mathrm{MEG}}$.

As Fig 3 shows, there are 12 dipole under different position, and are sorted in ascending order by each dipole's distance to the sphere core. The fitting average error of HPI and our system are 2.4131 mm and 2.4191 mm. The error of both systems are quite equivalent.

IV. Discussion

In MEG data acquisition stage, our work uses multiple feature points to be the input parameters for pose estimation. In reality, the fixed places of the subject's face are not to much, for example, nose tip, forehead. So it would be more feasible if we could decrease the number of feature points. We also are

Item	STD σ of Rotation(degree)	STD σ of Translation(m)
${}^{\mathrm{OBJ}}\mathrm{T}_{\mathrm{MEG}}$	$[0.2706, 0.1300, 0.0536]$	$[0.1153, 0.1691, 0.2680]$
${}^{\mathrm{CAM}}\mathrm{T}_{\mathrm{OBJ}}$	$[0.0041, 0.0030, 0.0012]$	$[0.0067, 0.0108, 0.0609]$
${}^{\mathrm{CAM}}\mathrm{T}_{\mathrm{MEG}}$	$[0.2700, 0.0714, 0.1207]$	$[0.1181, 0.2427, 0.2253]$

TABLE I
THE STABILITY OF THE ${}^{\mathrm{CAM}}\mathrm{T}_{\mathrm{MEG}}$.

Item	STD σ of MEG HPI's ${}^{\mathrm{HEAD}}\mathrm{T}_{\mathrm{MEG}}$	STD σ of our system's ${}^{\mathrm{HEAD}}\mathrm{T}_{\mathrm{MEG}}$
$Rotation$ $[\alpha, \beta, \gamma]\,(^\circ)$	$[0.2706, 0.1300, 0.0536]$	$[0.0004, 0.0009, 0.0031]$
$Translation$ $[x, y, z]\,(mm)$	$[0.1153, 0.1691, 0.2680]$	$[0.0101, 0.0544, 0.0289]$

TABLE II
THE STABILITY OF THE MEG HPI AND OUR SYSTEM.

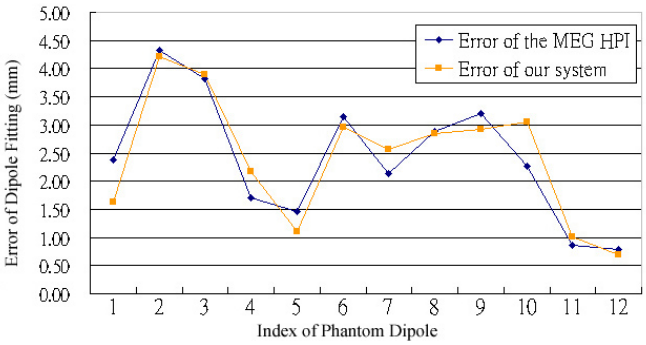

Fig. 3. Dipole fitting error. There are 12 dipoles under different position, and are sorted in ascending order by each dipole's distance to the sphere core. The average error of HPI and our system are 2.4131 mm and 2.4191 mm. The error of both systems are quite equivalent.

investigating efficiency and accuracy pose estimation method for better solution – [7] for example.

In our work, we define the $\mathrm{C}_{\mathrm{HEAD}}$ and $\mathrm{C}_{\mathrm{OBJ}}$ through the digitizer, which still has a little variance in the stability. In the future, we can use stereo camera to estimate coordinates of feature points. If MRI device is available, we can replace feature points by visible markers. After MRI scanning, it is able to obtain $\mathrm{C}_{\mathrm{OBJ}}$ and the coordinates of visible markers from 3D MRI data. Also, we can overlay the dipole position with 3D MRI data directly.

The location estimation of HPI is sensitive to the external noise, so the result of ${}^{\mathrm{HEAD}}\mathrm{T}_{\mathrm{MEG}}$ will be affected by external noise. According to our experience, we have to redo many times to look for a better HPI fitting results. From the results of Table II, our work is more stable than HPI, and is more resistible to the external noise.

The proposed method can estimate the position of the subject's head in the MEG device coordinate system during experiments without interfering with brain signals. In other words, we are able to do the online motion estimation such that we may monitor the status of the subject's head online. It is possible for suspending the experiment in time when the subject's head moves considerable away from the original position.

V. CONCLUSION

This paper presents a new coordinate system alignment technique without using HPI coils. According to the experiment results, we clearly demonstrate the feasibility, stability, and accuracy of the proposed camera-guided alignment method.

ACKNOWLEDGMENT

The authors gratefully appreciate Mr. Chih-Yu Cheng for his kindly help about MEG source modeling software. This research is partially sponsored by National Science Council (93-2815-C-009-001-E and 93-2213-E-010-006) and Taipei Veterans General Hospital (VGH 93-356-4).

REFERENCES

[1] M. Hamalainen, R. H. Risto, J. Ilmoniemi, J. Knuutila, and O. V. Lounasmaa, "Magnetoencephalography - theory, instrumentation, and applications to noninvasive studies of the working humans brain," *Reviews of Modern Physics*, vol. 65, no. 2, pp. 413–197, 1993.

[2] J. Knuutila, A. Ahonen, M. Hamalainen, R. Ilmoniemi, and M. Kajola, "Design considerations for multichannel squid magnetometers," in *SQUID'85: Superconducting Quantum Interference Devices and their Applications*, Walter de Gruyter, Berlin, Jun 1985, pp. 939–944.

[3] K. Uutela, S. Taulu, and M. Hamalainen, "Detecting and correcting for head movements in neuromagnetic measurements," *NeuroImage*, vol. 14, pp. 1424–1431, 2001.

[4] Z. Zhang, "A flexible new techique for camera calibtion," *IEEE Trans. Pattern Analysis and Machine Intelligence*, vol. 22, no. 11, pp. 1330–1334, 2000.

[5] Y.-S. Chen, Y.-P. Hung, and C.-S. Fuh, "Fast block matching algorithm based on the winner-update strategy," *IEEE Transactions on Image Processing*, vol. 10, no. 8, pp. 1212–1222, 2001.

[6] N. Otsu, "Threshold selection method from gray-level histograms," *IEEE Trans. Systems Man Cybernet*, vol. 9, no. 1, pp. 62–69, 1979.

[7] C.-P. Lu, G. D. Hager, and E. Mjolsness, "Fast and globally convergent pose estimation from video images," *IEEE Trans. Pattern Analysis and Machine Intelligence*, vol. 22, no. 6, pp. 610–622, 2000.